RESEARCH ARTICLE

Amyloid beta cleavage by ANA-TA9, a synthetic peptide from the ANA/BTG3 Box A region

Yusuke Hatakawa[1] | Rina Nakamura[2,3] | Motomi Konishi[4] | Toshiyasu Sakane[1] |
Akiko Tanaka[1] | Akira Matsuda[5] | Motoaki Saito[3] | Toshifumi Akizawa[2,3] (iD)

[1] Pharmaceutical Technology, Kobe Pharmaceutical University, Higashinada, Kobe, Japan

[2] O-Force Co., Ltd, Hata-gun, Kochi, Japan

[3] Laboratory of Pharmacology, School of Medicine, Kohasu, Oko-cho, Kochi University, Nankoku, Kochi, Japan

[4] Department of Integrative Pharmaceutical Science, Faculty of Pharmaceutical Sciences, Setsunan University, Hirakata, Osaka, Japan

[5] Laboratory of Medicinal and Biochemical Analysis, Faculty of Pharmaceutical Sciences, Hiroshima International University, Kure, Hiroshima, Japan

Correspondence
Toshifumi Akizawa, Ph. D. Laboratory of Pharmacology, School of Medicine, Kochi University, Kohasu, Oko-cho, Nankoku, Kochi 783-8505, Japan.
Email: momizit0510@gmail.com or jm–momizit@kochi-u.ac.jp

Abstract

Introduction: We recently discovered a short synthetic peptide derived from the ANA/BTG3 protein Box A region called ANA-TA9 (SKGQAYRMI), which possesses catalytic activity. Herein we demonstrated the proteolytic activity of ANA-TA9 against amyloid beta 42 (Aβ42).

Methods: The proteolytic activity of ANA-TA9 against both the authentic soluble form Aβ42 (a-Aβ42) and the solid insoluble form Aβ42 (s-Aβ42) was analyzed by high-performance liquid chromatography and mass spectrometry. Plasma clearance, brain uptake, and cell viability were examined.

Results: ANA-TA9 cleaved not only a-Aβ42 but also s-Aβ42. Proteolytic activity was partially inhibited by 4-(2-aminoethyl) benzenesulfonyl fluoride hydrochloride, a serine protease inhibitor. Plasma clearance was very rapid, and the brain concentration indicated efficient brain delivery of ANA-TA9 via nasal application. Cell viability analysis indicated that ANA-TA9 did not display toxicity.

Discussion: ANA-TA9 is an attractive potential candidate for the development of novel peptide drugs in Alzheimer's disease treatment.

KEYWORDS
administered nasally (i.n.), Alzheimer's disease, ANA/BTG3, Aβ fragment peptide, Aβ42, catalytide, neurodegenerative disease, serine protease, synthetic peptide

1 | BACKGROUND

We first reported on the proteolytic activity of a short synthetic peptide, JAL-TA9 (YKGSGFRMI), derived from the Box A region of Tob1 (Figure S1).[1] JAL-TA9 cleaved three types of amyloid beta (Aβ) fragment peptides, including Aβ11-29, which is derived from the central region and thought to be the core region for Aβ42 aggregation or oligomerization.[2] No reports on the catalytic activity of the short synthetic peptide were published prior to our serial studies on hydrolase-like peptides; therefore, we coined catalytide (catalytic peptide) as the general name of proteolytic peptides. In addition, 5-mer peptides derived from the active center of JAL-TA9 cleaved the

Aβ-fragment peptides.[3] These proteolytic activities were inhibited by the serine protease inhibitor 4-(2-aminoethyl) benzenesulfonyl fluoride hydrochloride (AEBSF).[1,4] Of interest JAL-TA9 cleaved the authentic soluble form Aβ42 (a-Aβ42) and the solid insoluble form Aβ42 (s-Aβ42), which cause Alzheimer's disease (AD) in the central region.[4] AD is well known as the most common age-related neurodegenerative disorder, and Aβ is predicted to be the most efficient target of drug therapies.[5–14] Many studies have been conducted to develop an AD treatment that targets Aβ42 degradation, clearance, and inhibition of aggregation or oligomerization; however, the results have not been promising, as all of the strategies thus far have failed in clinical trials.[13–18]

In the present study we successfully determined that the ANA-TA9 (SKGQAYRMI) sequences from the ANA/BTG3 protein Box A region corresponding to JAL-TA9 also possessed proteolytic activity and was composed of two kinds of catalytides (ANA-SA5: SKGQA and ANA-YA4: YRMI) (Figure S1).[19] However, we also observed two interesting differences between ANA-TA9 and JAL-TA9. One was the inhibitory effect of AEBSF. The proteolytic activity of JAL-TA9 was completely inhibited by AEBSF, but that of ANA-TA9 was only partially inhibited. The other was the number and position of cleavage sites on Aβ peptide fragments. It goes without saying that the cleavage mechanism must be clarified; however, ANA-TA9 and JAL-TA9 are two of the most attractive novel drug candidates not only for AD treatment but also for prevention.

Herein we presented the proteolytic activity of ANA-TA9 against both a-Aβ42 and s-Aβ42.

2 | METHODS

2.1 | Chemical synthesis of the peptides

ANA-TA9 and s-Aβ42 were synthesized from Fmoc-protected L-amino acid derivatives according to the method described previously[4,19,20] using an automated peptide synthesizer (model 433A; Applied Biosystems, Foster City, CA, USA) and a 0.1 mmol scale with preloaded resin. After deprotection according to the manufacturer's protocol, ANA-TA9 was purified using reversed-phase high-performance liquid chromatography (HPLC; Capcell Pak C18 column, SG, 10 or 15 i.d. × 250 mm; Shiseido Co., Ltd., Tokyo, Japan) with a linear elution gradient from 0.1% trifluoroacetic acid (TFA) to 50% or 70% CH$_3$CN containing 0.1% TFA over 30 minutes. The flow rate was set at 3 or 6 mL/min. The primary peak fractions were collected and lyophilized. The purity of the synthetic peptides and progress of the enzymatic reaction were confirmed by analytical reversed-phase HPLC (Capcell Pak C18 column, MGII, 4.6 i.d. × 150 mm; Shiseido Co., Ltd.) at a flow rate of 1.0 mL/min with a linear elution gradient from 0.1% TFA to 70% CH$_3$CN containing 0.1% TFA. The column eluate was monitored with a photodiode-array detector (SPD-M20A; Shimadzu, Kyoto, Japan). Each purified peptide was characterized by electrospray ionization mass spectrometry (ESI-MS) using the Qstar Elite Hybrid liquid chromatography (LC)-MS/MS system (Applied Biosystems).[1,3,4,19,20]

HIGHLIGHTS

- ANA-TA9 cleaves both authentic and soluble forms, respectively (a-Aβ42 and s-Aβ42) of amyloid beta 42.
- ANA-TA9 does not display toxicity.
- ANA-TA9 is a novel potential drug target for Alzheimer's disease (AD) treatment and prevention.

RESEARCH IN CONTEXT

1. **Systematic review**: The authors reviewed the literature using PubMed, Web of Science, and through meeting abstracts and presentations. We included our serial publications, which associate catalytides, or hydrolase-like peptides, with important new aspects for treating and preventing Alzheimer's disease (AD) pathophysiology.
2. **Interpretation**: This is the first study to demonstrate proteolytic activity against amyloid beta 42 (Aβ42) through animal experiments, including plasma clearance, brain uptake, and growth effects of ANA-TA9 A549 cells. The data obtained in this study suggest that ANA-TA9 is an attractive potential candidate for novel strategic drug development in AD treatment and prevention.
3. **Future directions**: Prospective clinical observations and validation in model systems are needed to develop novel drug treatments for AD.

The preparation of synthetic s-Aβ42, including deprotection and purification processes, is very difficult because Aβ42 is insoluble in most solvents except strong acids, such as TFA, and also polymerizes or aggregates, which interferes with AD studies. Thus we changed the deprotection and cleavage method conditions from those recommended by the manufacturer. A slightly brownish solid material, referred to as s-Aβ42, was obtained after lyophilization and continuously washed with CH$_3$CN and CH$_3$OH.[4]

2.2 | Analysis of proteolytic activity and determination of the cleavage sites

ANA-TA9 (final concentration: 0.2 mM) was individually incubated with or without the a-Aβ42 in the presence of human serum albumin (HSA; final concentration: 0.025% w/v) in phosphate-buffered saline (PBS; pH 7.4) at 37°C. A portion of the reaction mixture was analyzed in a time-dependent manner using the analytical HPLC system described in preceding text. The peak fractions monitored at 220 nm were collected in microtubes (Eppendorf Safe-Lock Tubes, 1.5 mL; Eppendorf,

Hamburg, Germany). After lyophilization, the appropriate quantity of 36% CH_3CN containing 0.1% HCOOH was determined based on the chromatographic peak height and added via stirring with an automatic mixer. The cleavage sites were determined by ESI-MS using the flow injection method with 70% CH_3CN containing 0.1% HCOOH on the Qstar Hybrid LC-MS/MS system (Applied Biosystems). The flow rate was set at 0.1 mL/min.

On the other hand, s-Aβ42 was incubated with or without ANA-TA9 and analyzed under the same conditions as a-Aβ42 after continuous washing with CH_3CN and CH_3OH to remove the amino acid protecting groups and other byproducts. Because s-Aβ42 was not dissolved in the reaction buffer, the experiment scale was set to five times larger than that of a-Aβ42 with the same ratios of all reagents.

2.3 | Animal studies

All animal experiments were conducted according to the principles and procedures outlined in the National Institutes of Health Guide for the Care and Use of Laboratory Animals (NIH publication #85-23). All animal experiment protocols were approved by the Animal Experiment Committee of Kobe Pharmaceutical University. Male Wistar/ST rats weighing 230-250 g for the examination of plasma clearance and male ddY mice weighing 25 g for the evaluation of brain uptake were purchased from Japan SLC (Shizuoka, Japan).

2.4 | Plasma clearance of ANA-TA9 following intravenous bolus injection

Male Wistar/ST rats were anesthetized with intraperitoneal pentobarbital sodium (52 mg/kg), and the right femoral artery was cannulated with polyethylene tubing. ANA-TA9 (10 mg/mL; 200 μL) was injected into the left femoral vein at a dose of 2 mg/head. At the appropriate time intervals, blood samples were collected and centrifuged at $5000 \times g$ for 5 minutes to obtain the plasma. The plasma samples were frozen and stored at $-40°C$ until the assay.

2.5 | Brain uptake of ANA-TA9 following intraperitoneal and nasal administration

The PBS solution of ANA-TA9 (100 mg/mL PBS) was administered intranasally (i.n.) via the left nostril of male ddY mice at a dose of 1 mg (10 μL). ANA-TA9 (10 mg/mL PBS) was administered intraperitoneally (i.p.) at the same dose of 1 mg (10 μL). Thereafter, blood was collected at 5, 15, and 30 minutes post-administration. After blood sampling at 30 minutes, the abdomen of each mouse was opened, and a saline and heparin solution was flushed by perfusion from the left cardioventricule to remove the blood from the cerebral blood vessel. The whole brain was removed and washed with ice-cold saline. The concentrations of ANA-TA9 in the plasma and brain were determined using LC/MS.

2.6 | ANA-TA9 assay

The plasma and brain concentrations of ANA-TA9 were determined using the LC-20A and LCMS-2020 instruments (Shimadzu). Briefly, 100 μL of plasma was mixed with 1000 μL of methanol. The mixture was centrifuged, and the supernatant was evaporated until dry. Separately, 100 μL of purified water was added to the brain section, and the mixture was homogenized. To the homogenate, 4000 μL of methanol was added. The mixture was centrifuged, and the supernatant was evaporated until dry. The evaporated samples from the plasma and brain were reconstituted with 100 μL of the mobile phase. Chromatographic separation was performed using a C18 analytical column (TSKgel ODS 100V, 3 μm, 2.0 mm inner diameter (i.d.) × 100 mm; TOSOH, Tokyo, Japan). The mobile phase was acetonitrile:0.1% acetic acid = 10/90 (v/v), and the flow rate was 0.2 mL/min. ANA-TA9 eluted from the column was analyzed in positive mode. Other conditions (temperatures and voltages) were maintained at the default settings. Nitrogen was used as the nebulization gas at a flow rate of 1.5 L/min.

2.7 | Effect of ANA-TA9 on the growth of A549 cells

Cisplatin (CDDP) was purchased from FUJIFILM Wako Pure Chemical Corporation (Osaka, Japan). WST-8 (Cell Counting Kit-8) was purchased from Dojindo Laboratories (Kumamoto, Japan). The FLAG peptide (DYKDDDDK) was purchased from Sigma-Aldrich (St. Louis, MO, USA). The human lung cancer cell line A549 was obtained from Riken Cell Bank (Ibaraki, Japan). A549 cells were maintained in Dulbecco's Modified Eagle Medium (DMEM) supplemented with 10% fetal bovine serum, 100 units/mL penicillin, and 100 μg/mL streptomycin at 37°C in a humidified atmosphere of 5% CO_2. Cell viability was evaluated using the WST-8 method. A549 cells were seeded into 96-well plates (4×10^3 cells/well). After incubation for 24 hours, the medium was replaced, and the cells were treated with 0.2 mM ANA-TA9, 0.2 mM FLAG peptide, and 4 μM CDDP. After incubation for 72 hours, the medium was replaced with 110 μL of medium containing WST-8 reagent (10 μL WST-8 reagent and 100 μL DMEM). The cells were further incubated for 1 hour, and the absorbance was determined at 450 nm with a reference wavelength of 620 nm using a SpectraMax Plus384 microplate reader (Molecular Devices, Sunnyvale, CA, USA).

3 | RESULTS

3.1 | Proteolysis of a-Aβ42 by ANA-TA9

We first examined the proteolytic activity of ANA-TA9 to a-Aβ42 purchased from the Peptide Institute (Osaka, Japan) in PBS (pH 7.4) with HSA at 37°C.[4] The reaction mixtures of ANA-TA9 and a-Aβ42 were analyzed every day up to 7 days (Figure 1A). ANA-TA9 was initially eluted as a single peak at ≈10 minutes, and a-Aβ42 was co-eluted with HSA at around ≈13 minutes. On day 1, ANA-TA9 completely
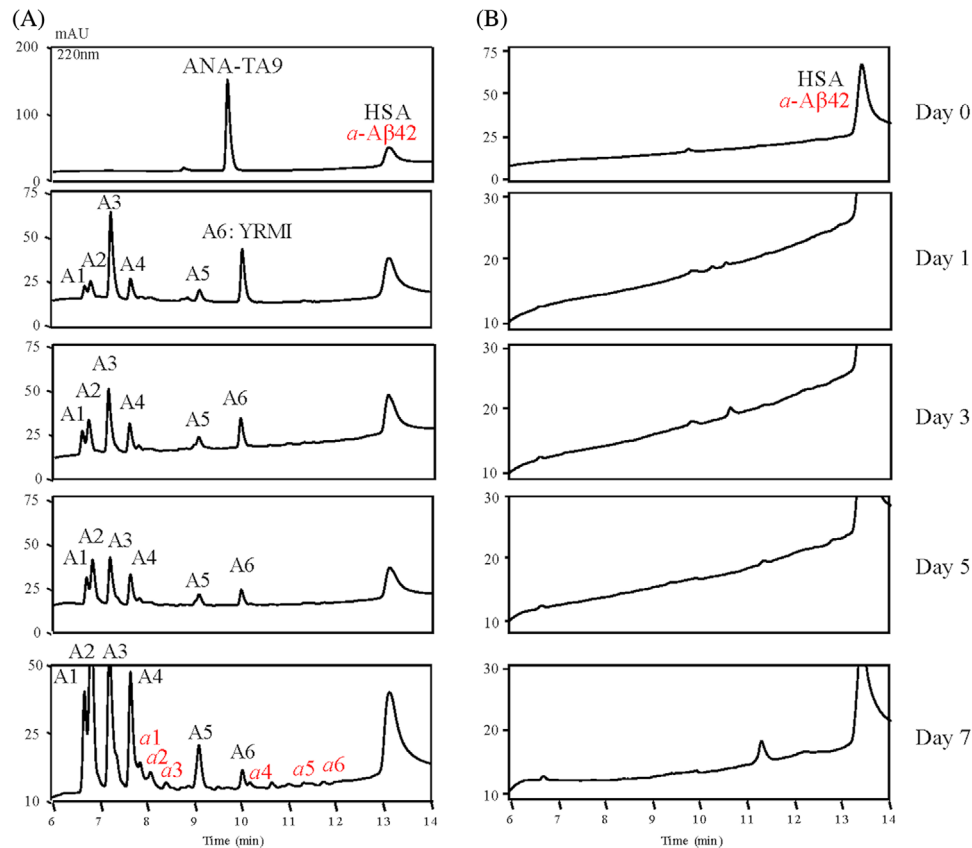
FIGURE 1 Cleavage reaction of the authentic soluble form amyloid beta 42 (a-Aβ42) by ANA-TA9. Aβ42 (final concentration: 0.05 mM) was incubated in presence of human serum albumin (HSA; final concentration: 0.025% w/v) in phosphate-buffered saline at 37°C with (A) or without ANA-TA9 (B). From day 0 to day 7, 10 μL of the reaction mixture was analyzed by high-performance liquid chromatography. After 7 days, 20 μL of the reaction mixture was injected, and all of the new peaks were collected. A1-A6 and a1-a6 were identified as the fragment peptides of ANA-TA9 and a-Aβ42, respectively (Table 1A)

disappeared, and six types of peaks (A1-A6) were observed. Of interest, the chromatogram patterns, especially the comparative heights of individual peaks, were changing up to day 7 after ANA-TA9 disappeared. ANA-TA9 consists of two different catalytic peptides: YRMI (ANA-YA4) and SKGQA (ANA-SA5).[19] The chromatogram changing after ANA-TA9 disappeared might be due to the cleavage reaction against a-Aβ42 by these two proteolytic peptides produced from ANA-TA9. In the case of a-Aβ42 alone, no fragment peptide was identified (Figure 1B). On day 7, all appearing peaks were collected (Figure 1A), and eight kinds of peptides from six peaks (a1-a6) were identified as Aβ42-derived fragments (Table 1A). To calculate the decreasing ratio of a-Aβ42, Aβ36-42 (a4: VGGVVIA) on the chromatogram (Figure 1A) was synthesized as the standard peptide because the amino acid sequence of Aβ36-42 was not identified in another fragment peptide. As a result, the decreasing ratio of a-Aβ42 was calculated as 12% after 7 days of incubation (Figure S3 in Supporting Information).

3.2 | Proteolysis of s-Aβ42 by ANA-TA9

We next examined the proteolytic activity of ANA-TA9 against s-Aβ42 prepared by ourselves in PBS (pH 7.4) with HSA at 37°C.[4] Because

s-Aβ42 was not dissolved in the reaction buffer, it was not initially identified. ANA-TA9 appeared as a single peak on day 0. The auto-proteolytic reaction of ANA-TA9 was observed on day 1 similar to a-Aβ42 (Figure 1). Time-dependent analysis of the reaction mixture indicated that the cleavage reaction continuously progressed up to 7 days (Figure 2). Thus we collected all appearing peaks on day 7, and 21 peptides were identified as fragments derived from s-Aβ42 (Figure 2A and Table 1B). On the other hand, in the case of s-Aβ42 alone, only four peptides were identified on day 7 (Figure 2B and Table 1C), although there is no peak on day 0. These four peptides contained the Ala residue of the C-terminal end in Aβ42 and might possess the insoluble character similar to s-Aβ42. In addition, these peptides were also identified in the reaction mixture co-incubated with ANA-TA9. Taken together, we concluded that these four peptides were not products by cleavage reaction but by-products of Aβ42 synthesis process.

Of interest, the s-Aβ42 figure changed after coincubation with ANA-TA9 for 7 days (Figure 2C). In this case, the weight of s-Aβ42 also decreased from 0.30 mg on day 0 to 0.22 mg after coincubation with ANA-TA9 for 7 days. The decreasing ratio of s-Aβ42 was calculated to be 27%. On the other hand, when s-Aβ42 was incubated in the absence of ANA-TA9, the weight of s-Aβ42 decreased from 0.30 mg on day 0

TABLE 1 Mass spectrometry (MS) analyses of the reaction mixture of a-Aβ42 (A) and the solid insoluble form s-Aβ42 (B and C)

(A)			
Peak	Fragment	Theoretical MS	Experimental MS
A1	YR	337.18	337.1731
	I	131.09	131.0942
A2	Y	181.07	181.0724
	RM	305.15	305.1610
A3	SKGQAYR	808.42	808.4268
A4	SKGQAY	652.32	652.3095
A5	MI	262.14	262.1355
A6	YRMI	581.30	581.3140
a1	YEVH	546.24	546.2572
	HQKL	524.31	524.3210
a2	DAEFRH	773.35	773.3640
a3	DAEFR	636.29	636.2833
a4	VGGVVIA	613.38	613.3832
a5	VFFA	482.25	482.2516
	EDVGSNKGAIIGLM	1402.71	1402.7366
a6	IIGLM	545.32	545.3267
(B)			
Peak	Fragment	Theoretical MS	Experimental MS
A1	YR	337.18	337.1838
	I	131.09	131.0942
A2	Y	181.07	181.9785
	RM	305.15	305.1610
A3	SKGQAYR	808.42	808.4556
A4	SKGQAY	652.32	652.3426
A5	YRM	468.22	468.2980
A6	MI	262.14	262.1374
A7	ANA-TA9	1052.54	1052.5574
A8	YRMI	581.30	581.3567
s1	SGYE	454.17	454.2863
s2	YEV	409.18	409.2268
	HDSGY	577.21	577.2943
s3	RHDSGYE	862.36	862.3662
s4	EFRH	587.28	587.3010
	FRH	458.24	458.2579
s5	AEFRHDSGY	1080.46	1080.5766
	KLVFFAE	852.47	852.4496
s6	RHDSGY	733.31	733.4028
	VVIA	400.27	400.2698
	GGVVIA	514.31	514.3103
s7	FAEDVGSNK	965.45	965.5390
	GVVIA	457.29	457.2901
	VGGVVIA	613.38	613.3732
s8	KGAIIGL	670.44	670.4088
	LVFFAE	724.38	724.3462
s9	VHH	391.20	391.2900
s10	LMVGGVVI	786.47	786.4394

(Continues)

TABLE 1 (Continued)

(B)			
Peak	Fragment	Theoretical MS	Experimental MS
s11	VFFAEDV	825.39	825.3709
	DVGSNKGAII	972.52	972.5461
	EVHHQKLVFFAED	1597.79	1597.9410
(C)			
Peak	Fragment	Theoretical MS	Experimental MS
b1	GGVVIA	514.31	514.4486
	VVIA	400.27	400.3619
b2	GVVIA	457.29	457.4021
b3	VGGVVIA	613.38	613.5443

Cleavage sites were determined by electrospray ionization (ESI)-MS using flow injection methods on the Qstar Hybrid LC-MS/MS system (Applied Biosystems, Foster City, CA, USA).
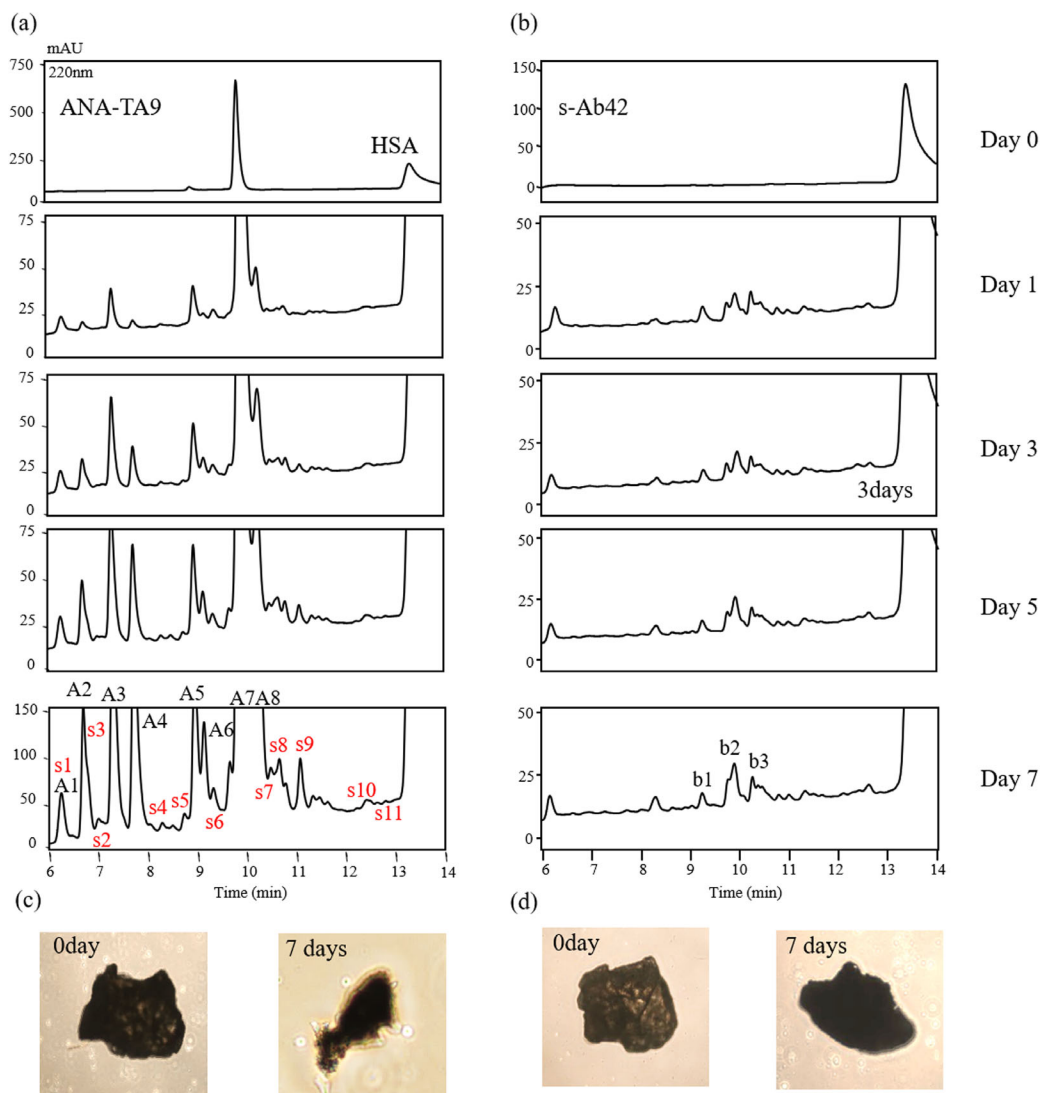

FIGURE 2 Cleavage reaction of s-Aβ42 by ANA-TA9. s-Aβ42 (0.3 mg) was incubated with (A) or without (B) ANA-TA9 (final concentration: 1 mM) in the presence of HSA (final concentration: 0.125% w/v) in PBS at 37°C. From day 0 to day 7, 10 μL of the reaction mixture was analyzed by HPLC. After 7 days, 100 μL of the reaction mixture was injected, and all of the new peaks were collected. A1-A8 and s1-s11 were identified as the fragment peptides of ANA-TA9 and s-Aβ42, respectively (Table 1B). (C) Photo of s-Aβ42 co-incubated with (C) or without (D) ANA-TA9 after 0 and 7 days

a-Aβ42

^{1}DAEFRHDSGYEVHHQKLVFFAEDVGSNKGAIIGLMVGGVVIA^{42}

s-Aβ42
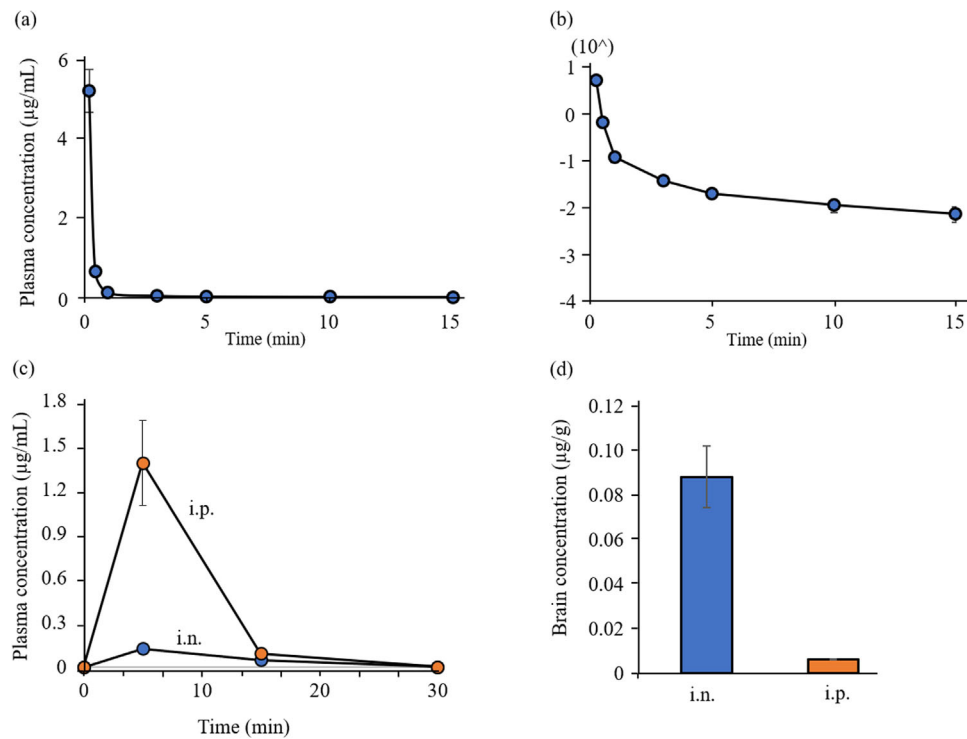
FIGURE 3 Comparison of cleavage sites

FIGURE 4 Plasma clearance and brain uptake of ANA-TA9. The time-concentration profiles of ANA-TA9 in the plasma following intravenous bolus injection plotted on normal (A) and semilogarithmic scales (B). The profiles of ANA-TA9 concentration in the plasma (C) and brain (D) at 30 minutes following nasal and intraperitoneal application to mice

to 0.25 mg after 7 days, and the decreasing ratio was calculated to be 17% (Figure 2D). Considering these findings together, the decreasing ratio of s-Aβ42 by ANA-TA9 was calculated to be 10% over 7 days.

3.3 | Comparison of cleavage sites

The cleavage sites on both a-Aβ42 and s-Aβ42 by ANA-TA9 were determined on the basis of MS analyses (Figure 3). Overall, the number of s-Aβ42 cleavage sites of s-Aβ42 are a lot by comparison with a-Aβ42. Of interest, ANA-TA9 mainly cleaved the central region of a-Aβ42. On the other hand, many cleavage sites were identified on the N-terminus and C-terminus of s-Aβ42. The difference of the cleavage site between a-Aβ42 and s-Aβ42 was probably caused by stereo-structural differences of substrate. These results were similar to JAL-TA9.[4]

3.4 | Plasma clearance

We next analyzed the concentration of ANA-TA9 in the plasma following intravenous bolus injection (Figure 4A and B). The profiles

indicated that the plasma clearance was very rapid with an initial half-life of 10 seconds. The concentration within 15 minutes post-injection was below the detection limit. These findings clearly suggest that ANA-TA9 delivery to the brain through the blood-brain barrier (BBB) is very difficult. ANA-TA9 is rapidly cleared from the blood before enough can be taken up by the brain through the BBB. According to the area under the curve (AUC) of ANA-TA9 (7.41 ± 1.31 μg min/mL), the total body clearance was calculated as 270 mL/min. This value was surprisingly higher than the body clearance of many drugs that undergo normal urinary excretion and/or hepatic metabolism.

3.5 | Brain uptake after intranasal and intraperitoneal administration

We next analyzed the concentration of ANA-TA9 in the plasma and brain for 30 minutes after administration. The concentration of ANA-TA9 in the plasma following intranasal administration was lower than that after intraperitoneal administration (Figure 4C). The AUC up to 30 minutes after nasal administration (1.63 ± 0.03 μg min/mL) was only 14% of that after intraperitoneal administration (11.6 ± 2.1 μg
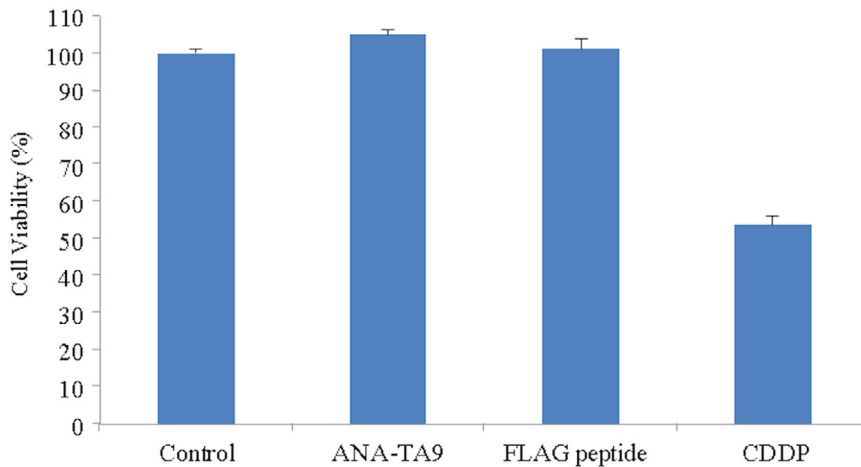
FIGURE 5 Effect of ANA-TA9 on the growth of A549 cells. Cell viability was evaluated by the Cell Counting Kit-8 (WST-8) method. The cells were seeded into 96-well plates (4×10^3 cells/well) and treated with 0.2 mM ANA-TA9, 0.2 mM FLAG peptide, and 4 μM cisplatin. After 72 hours, the absorbance at 450 nm was measured using WST-8 reagent

min/mL). On the contrary, the brain concentration within 30 minutes after intranasal administration was 1467% higher than that after intraperitoneal administration, indicating the efficient brain delivery of ANA-TA9 by nasal application (Figure 4D).

3.6 | Effect of ANA-TA9 on the growth of A549 cells

To determine the cell toxicity of ANA-TA9, we examined its effect on the growth of A549 cells (Figure 5). ANA-TA9 (0.2 mM) did not show a significant inhibitory effect on the growth of A549 cells compared to the FLAG peptide, which was used as a peptide control. On the other hand, chemotherapeutic agent CDDP, which was used as a positive control, inhibited the growth of A549 cells.[21]

4 | DISCUSSION

Aggregation and accumulation of Aβ42 is known to be a primary cause of AD, and the Aβ42 oligomer has shown strong neurotoxicity. This study suggests that ANA-TA9 may cleave not only aggregated Aβ42 but also oligomeric Aβ42 and thus constitutes a novel potential peptide target for AD drug treatment as well as JAL-TA9.[4] In terms of clinical application, what is important to determine is side effects, such as cleavage reactions against various major proteins, in vivo stability, and administration method.

We previously reported that ANA-TA9 did not cleave five native proteins, specifically HSA, γ-globulin, rabbit immunoglobulin G, cytochrome C, and lysozyme.[19] These results strongly suggest that ANA-TA9 does not result in severe side effects. The in vitro stability of ANA-TA9 in plasma and whole blood is not particularly labile (data not shown). Furthermore, ANA-TA9 is likely degraded on the surface of endothelial cells, possibly after rapidly binding to them.

Many authors have reported on direct drug delivery to the brain via nasal application. Our previous articles have clarified the efficient nasal delivery of oxytocin and CPN-116 (the agonist peptide of type 2 neuromedin U receptor) to the brain.[22,23] Nasal application of ANA-TA9

may allow for the development of novel therapeutic systems to treat AD and dementia.

The ANA/BTG3 protein was initially identified as a novel antiproliferative agent based on its homology to the Tob gene.[24] Although there have been many reports about the Tob/BTG family of proteins, the functions of their three regions are still not well understood. Therefore, the mechanism underlying cleavage reactions remains unclear. The stereo-structure of ANA-TA9 estimated with use of computer analyses suggests that its cleavage mechanism may be similar to that of JAL-TA9.[4]

5 | CONCLUSION

This study proved that 9-mer synthetic peptide ANA-TA9 derived from the ANA/BTG3 protein Box A region cleaves both soluble form a-Aβ42 and insoluble form s-Aβ42 via proteolysis. In addition, a sufficient amount of ANA-TA9 can be delivered to the brain via nasal application. Furthermore, animal experiments and cell viability analysis indicated that ANA-TA9 is likely nontoxic and safe for clinical use. Given these findings, we conclude with confidence that ANA-TA9 as well as JAL-TA9 are attractive candidates for the development of novel peptide drugs that may be clinically applicable to AD prevention and treatment without serious side effects.

AUTHOR CONTRIBUTIONS
Y.H., R.N., and T.A. were responsible for the experimental design and data interpretation. T.A., R.N., and Y.H. contributed mainly to writing and review of the manuscript. R.N. and Y.H. conducted all of the experiments, including the HPLC analyses and determination of cleavage sites. Y.H., R.N., and M.K. contributed to the MS analyses. Y.H., A.T., and T.S. contributed to the animal experiments. A.M. contributed to the cell experiments.

COMPETING INTEREST

The authors declare no conflicts of interest.

ORCID

Toshifumi Akizawa https://orcid.org/0000-0002-3440-0905

REFERENCES

1. Nakamura R, Konishi M, Taniguchi M, Hatakawa Y, Akizawa T. The discovery of shorter synthetic proteolytic peptides derived from Tob1 protein. *Peptides*. 2019;116:71-77.
2. Vivekanandan S, Brender JR, Lee SY, Ramamoorthy A. A partially folded structure of amyloid-beta (1-40) in an aqueous environment. *Biochem Biophys Res Commun*. 2011;411:312-316.
3. Nakamura R, Konishi M, Higashi Y, Saito M, Akizawa T. Comparison of the catalytic activities of 5-mer synthetic peptides derived from Box A region of Tob/BTG family proteins afainst the amyloid-beta fragment peptides. *Integrative Molecular Medicine*. 2019;6:1-4.
4. Nakamura R, Konishi M, Hatakawa Y, Saito M, Akizawa T. The novel catalytic peptide, a synthetic nona-peptide (JAL-TA9) derived from Tob1 protein, digests the amyloid-β peptide. *J Royal, Sci*. 2019;1(2):30-35.
5. Sun X, Chen WD, Wang YD. The key peptide in the pathogenesis of Alzheimer's disease. *Front Pharmacol*. 2015;6:221.
6. Karran E, Mercken M, De StrooperB. The amyloid cascade hypothesis for Alzheimer's disease: an appraisal for the development of therapeutics. *Nat Rev Drug Discov*. 2011;10(9):698-712.
7. Ahmed M, Davis J, Aucoin D, et al. Structural conversion of neurotoxic amyloid-β 1-42 oligomers to fibrils. *Nat Struct Mol Biol*. 2010;17(5):561-567.
8. Hamley IW. The amyloid beta peptide: a chemist's perspective. role in Alzheimer's and fibrillization. *Chem Rev*. 2012;112:5147-5192.
9. Lührs T, Ritter C, Adrian M, et al. 3D structure of Alzheimer's amyloid-β(1-42) fibrils. *Proc Natl Acad Sci U S A*. 2005;102(48):17342-17347.
10. Esler WP, Wolfe MS. A portrait of Alzheimer secretases - New features and familiar faces. *Science (80-)*. 2001;293:1449-1454.
11. Kotler SA, Brender JR, Vivekanandan S, et al. High-resolution NMR characterization of low abundance oligomers of amyloid-β without purification. *Sci Rep*. 2015;5:1-12.
12. Kotler SA, Walsh P, Brender JR, Ramamoorthy A. Differences between amyloid-β aggregation in solution and on the membrane: insights into elucidation of the mechanistic details of Alzheimer's disease. *Chem Soc Rev*. 2014;43(19):6692-6700.
13. Doody RS, Thomas RG, Farlow M, et al. Phase 3 trials of solanezumab for mild-to-moderate alzheimer's disease. *N Engl J Med*. 2014;370:311-321.
14. Sato T, Kienlen-Campard P, Ahmed M, et al. Inhibitors of amyloid toxicity based on β-sheet packing of Aβ40 and Aβ42. *Biochemistry*. 2006;45(17):5503-5516.
15. Kumar J, Namsechi R, Sim VL. Structure-based peptide design to modulate amyloid beta aggregation and reduce cytotoxicity. *PLoS One*. 2015;10(6):1-18.
16. Young LM, Saunders JC, Mahood RA, et al. Screening and classifying small-molecule inhibitors of amyloid formation using ion mobility spectrometry-mass spectrometry. *Nat Chem*. 2015;7:73-81.
17. Crouch PJ, Tew DJ, Du T, et al. Restored degradation of the Alzheimer's amyloid-β peptide by targeting amyloid formation. *J Neurochem*. 2009;108:1198-1207.
18. Storr T, Merkel M, Song-Zhao GX, et al. Synthesis, characterization, and metal coordinating ability of multifunctional carbohydrate-containing compounds for Alzheimer's therapy. *J Am Chem Soc*. 2007;129(23):7453-7463.
19. Hatakawa Y, Nakamura R, Konishi M, Sakane T, Saito M, Akizawa T. Catalytides derived from the Box A region in the ANA/BTG3 protein cleave amyloid-β fragment peptide. *Heliyon*. 2019;5(9):e02454. https://doi.org/10.1016/j.heliyon.2019.e02454.
20. Kojima A, Konishi M, Akizawa T. Prion fragment peptides are digested with membrane type matrix metalloproteinases and acquire enzyme resistance through Cu2+-binding. *Biomolecules*. 2014;4(2):510-526.
21. Horibe S, Matsuda A, Tanahashi T, et al. Cisplatin resistance in human lung cancer cells is linked with dysregulation of cell cycle associated proteins. *Life Sci*. 2015;125:31-40.
22. Tanaka A, Furubayashi T, Arai M, et al. Delivery of Oxytocin to the Brain for the Treatment of Autism Spectrum Disorder by Nasal Application. *Mol Pharm*. 2018;15(3):1105-1111.
23. Tanaka A, Takayama K, Furubayashi T, et al. Transnasal Delivery of the Peptide Agonist Specific to Neuromedin-U Receptor 2 to the Brain for the Treatment of Obesity. *Mol Pharm*. 2020;17(1):32-39.
24. Winkler GS. The mammalian anti-proliferative BTG/Tob protein family. *J Cell Physiol*. 2010;222:66-72.

SUPPORTING INFORMATION

Additional supporting information may be found online in the Supporting Information section at the end of the article.